An Electrochemical Characterisation of Silica-Zirconia Oxide Nanostructured Materials for Fuel Cells

Rudzani Sigwadi *, Touhami Mokrani, Fulufhelo Nemavhola

Posted Date: 27 September 2024

doi: 10.20944/preprints202409.2181.v1

Keywords: mesoporous silica; tetraethyl orthosilicate; nanoparticles; cyclic voltammetry

Article

An Electrochemical Characterisation of Silica-Zirconia Oxide Nanostructured Materials for Fuel Cells

Rudzani Sigwadi [1,*], Touhami Mokrani [2] and Fulufhelo Nemavhola [3,4]

[1] Department of Chemical and Materials Engineering, University of South Africa, Private Bag X6, Florida, 1710, South Africa
[2] ICAES, University of South Africa, Private Bag X6, Florida, 1710, South Africa
[3] College of Graduate Studies, University of South Africa, Private Bag X6, Florida, 1710, South Africa
[4] Department of Mechanical Engineering, Durban University of Technology, Durban, South Africa
* Correspondence: sigwara@unisa.ac.za

Abstract. The effect of zirconium modified with silica dioxide in the conductivity of modified nanocomposite membrane in proton exchange membrane fuel cells (PEMFCs) application. In this study silica-zirconia nanoparticles were successful synthesized by precipitation method. The surface area and surface morphology of Si-ZrO_2 nanoparticles were observed under BET analysis, X-ray diffraction (XRD), scanning electron microscope (SEM), and transmission electron microscope (HRTEM). SEM and XRD results show that silica was well incorporated into ZrO_2 nanoparticles with the mixed shape of nanorods and nanosphere. HRTEM shows a crystallised small nanoparticle with average diameter about 5–8 nm. The element analysis (EDX) confirms the presence of silica and zirconia nanoparticles as well as oxygen on the surface. The addition of silica has impact on the surface area and pore size of Si-ZrO_2 nanoparticles, with Si-ZrO_2 nanoparticles having a higher surface area of 185 m^2/g when calcinated at 600 °C. It was shown that the Si-ZrO_2 can be used as an impregnating membrane to enhance the conductivity as observed by cyclic voltammetry (CV), with a rectangular shape that exhibiting the best capacitance behaviour.

Keywords: mesoporous silica; tetraethyl orthosilicate; nanoparticles; cyclic voltammetry

1. Introduction

Nanotechnology has become an important field of study due to the unique chemical, biological, electrical, optical and magnetic properties of nanomaterials [1]. Because the field of nanotechnology has so many uses, such as dental care, biological sensors, medical imaging, assays, diagnostic kits, athletic gear, sunscreens, cosmetics, environmental cleanup, textiles, and gene inactivation, many researchers focus on this field of study [1]. The growth of nanotechnology has enabled researchers to look for new materials and modify already-existing materials to create new procedures. One such approach is the levitation technique, which is a cheap, efficient, reasonably easy, and adaptable method of making materials [2]. Materials of sizes between 1 and 100 nanometres are known as nanoparticles and have special characteristics that distinguish them from bulk materials [3,4]. Their improved surface-to-volume ratio, quantum effects and altered chemical and physical properties on a nanoscale are the sources of these properties [5,6]. Oxide compounds are not conductive to electricity; however, certain perovskite structured oxides are electronically conductive, finding application in the cathode of solid oxide fuel cells and oxygen generation systems. They are insoluble in aqueous solution and extremely stable making them useful in ceramic structure and light weight structural components in aerospace and electrochemical application such as fuel cell in which they exhibit ionic conductivity. Zirconia Oxide (ZrO_2) finds extensive applications in a variety of fields including biological fields (e.g., biosensors, cancer treatment, hip replacement), optical coatings, solar cells, fuel cells, dentist, oxidation selectivity, and catalysts [5,7,8–10]. Numerous applications find zirconia appealing due to its exceptional qualities, including

 doi:10.20944/preprints202409.2181.v

its redox, acid-basic, and chemical stability as well as its mechanical resistance [5,7], high surface to volume ratio and small size [8–10]. With a high melting temperature of 2750 °C, which makes it valuable as a refractory material, ZrO_2 has a special combine of features that set it apart from all other ceramic materials [11]. Because of the low thermal conductivity of zirconia, it is a suitable choice for thermal protection coatings and insulation materials in high temperatures [12]. Zirconia is high hardness and strength and is a durable material for applications that require mechanical stress resistance. ZrO_2 can be also used as additives to enhance the material's performance of materials, drug delivery and medical imaging due to their biocompatibility [13]. Zirconia is a ceramic material that exhibits interesting properties, including small size high ionic conductivity for oxygen ions. This property makes it useful in applications related to oxygen sensing and high-temperature fuel cells [14].

Zirconia is a special high-temperature solid electrolyte because it forms a defect structure with oxygen ion vacancy upon doping with specific aliovalent oxides. This significantly increases oxygen ion conductivity [11]. Moreover, zirconia can provide good ionic conductivity and thermochemical stability when doped with different transition metal cations [15] and showed the possibility of electrochemical measurement using solid-state galvanic cells based on zirconium solid electrolytes [16]. Mesoporous silica has a high surface and well-defined pore structure, ensuring sufficient active sites for catalytic reactions, adsorption processes, and drug delivery applications [17]. The combination of mesoporous silicon and zirconium oxide nanoparticles can achieve an optimal balance between surface, conductivity, stability, pore size distribution and mechanical stability, making it very useful for various applications such as electrical equipment, sensors, catalyst supports and solar cells [7].

2. Experiment

2.1. Materials

Sodium hydroxide pellets (NaOH) (Sigma-Aldrich), ethanol (Sigma-Aldrich), zirconium oxychloride hydrate ($ZrOCl_2$.$8H_2O$) (Sigma-Aldrich), Tetraethyl orthosilicate (TEOS) (Sigma-Aldrich, 98% purity), potassium chloride (KCl) (Sigma-Aldrich), Nafion® solution, D521-Alcohol based 1100 EW at 5 wt.% (Ion Power) and silver nitrate ($AgNO_3$) (Sigma-Aldrich).

2.2. Preparation of ZrO_2 Nanoparticles

The silica-zirconia oxide (Si-ZrO_2) synthesized by the precipitation method. 0.2M $ZrOCl_2.8H_2O$ and 2N NaOH were mixed in 250 ml glass beaker and stirred with magnetic stirrer for 2 hrs [18,19]. Silica precursor which is Tetraethoxysilane (TEOS) added to the obtained precipitate. TEOS added dropwise, and the mixture allowed to stir for 5 hrs. The resultant precipitate put for 24 hrs in the oven at 150 °C then centrifuged and washed with deionized water to remove all traces of chlorine ions (Cl^-). Then dried at 100 °C for 24 hrs, calcined at 600 °C for 2 hours [18,19] and named: Si-ZrO_2.

2.3. Characterization

The Brunauer-Emmett-Teller (BET), X-ray diffractometer (XRD), scanning electron microscopy (SEM), high-resolution transmission electron microscopy (HRTEM), thermogravimetric analysis (TGA), and Fourier transform infrared (FTIR) spectroscopy were used to characterised silica-zirconia nanoparticles.

2.4. Electrochemical Measurements

The three electrodes used for the electrochemical experiments. The silver-silver chloride (Ag/AgCl) as reference electrode, Si-ZrO_2 nanoparticles coated on glassy carbon as working electrode, and Pt wire as counter electrode. The working electrodes were prepared by ultrasonic mixing of 0.03 g Si-ZrO_2 and Nafion® solution (0.5 ml) and absolute ethanol for 30-minutes. The obtained solution was piped to the working electrode and

 doi:10.20944/preprints202409.2181.v

dried [20]. For electrochemical measurements, 2M of KCl solution were prepared. To observe the reaction behaviour of Si-ZrO_2 nanoparticles, the Cyclic voltage meters (CV) were conducted at various scanning rates of 100, 50, 30, 20 and 10 mV/s. Electrochemical impedance spectroscopy (EIS) measured the charge transfer properties of nanoparticles at frequencies from 100 kHz to 0.01 Hz.

3. Results and Discussion

3.1. The High-Resolution Transmission Electron Microscopy

The HRTEM images for Si-ZrO_2 nanoparticles are presented in Figure 1. The results obtained of Si-ZrO_2 nanoparticles has a mixture of spherical and rods like shape as shown in Figure 1 (a–d) with a nanometre's sizes range between 2 to 5 nm. Figure 1(a-d) reveals that ageing the Si-ZrO_2 nanoparticles at a higher temperature resulted in a smaller crystal size nanoparticles that are less than 2 nm [18–20], compared to 27 nm obtained by Kocjan et.al [21], this may due to the synthesis temperature. The selected area electron diffraction (SAED) pattern for Si-ZrO_2 is represented in Figure 2. The SAED pattern reflect the higher crystallising (1 1 1) for the monoclinic plane [18]. The concentric circles and clear scattering spots in Figure 2 may be due to the sample crystallisation. HRTEM images and lattice spacing of Si-ZrO_2 nanoparticles are showed in Figure 3. Figure 3 revealed that zirconia synthesis with silica obtain a very crystallised nanoparticles with a well oriented and define lattice fringes. The spacing between the lattice fringes was found to be 0.5343 nm which confirmed by XRD monoclinic structure of (111) plane, indicating that silicon doping can also affect the lattice properties of zirconium nanoparticles. In contrast, Lestari et al. obtained a distance between the fringes of 0.329 nm on zircon nanopowder [22]. The lattice spacing of high-crystalline nanoparticles is consistent with the predicted value of typical monoclinic ZrO_2 structures as shown in Figure 3 [23]. The obtained high crystallised Si-ZrO_2 nanoparticles it will be a good inorganic nanofiller for Nafion membrane which could enhance the performance in fuel cell application. EDAX results in Figure 4 demonstrate that the main elemental composition of Si-ZrO2 nanoparticles is silicon (S) at 14.6%, zirconium (Zr) at 1.2%, and oxygen (O) at 83.7%. The EDAX results confirmed that nanoparticles were more than 99.5% pure, and that the purity of nanoparticles was consistent with the synthesis method.

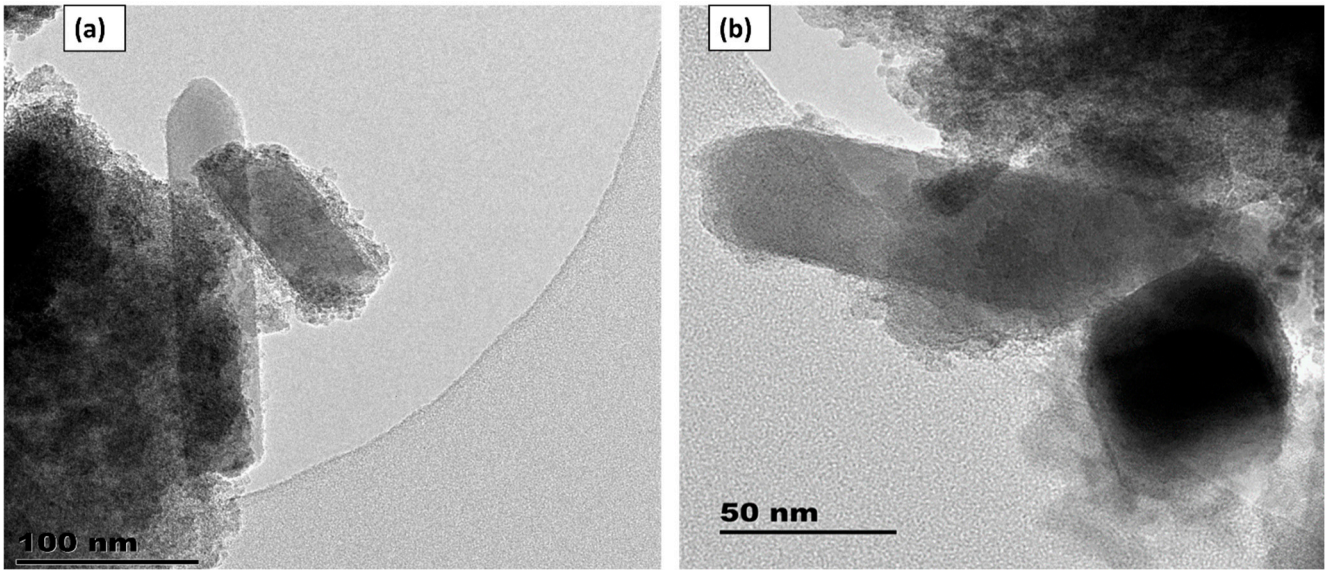

 doi:10.20944/preprints202409.2181.v

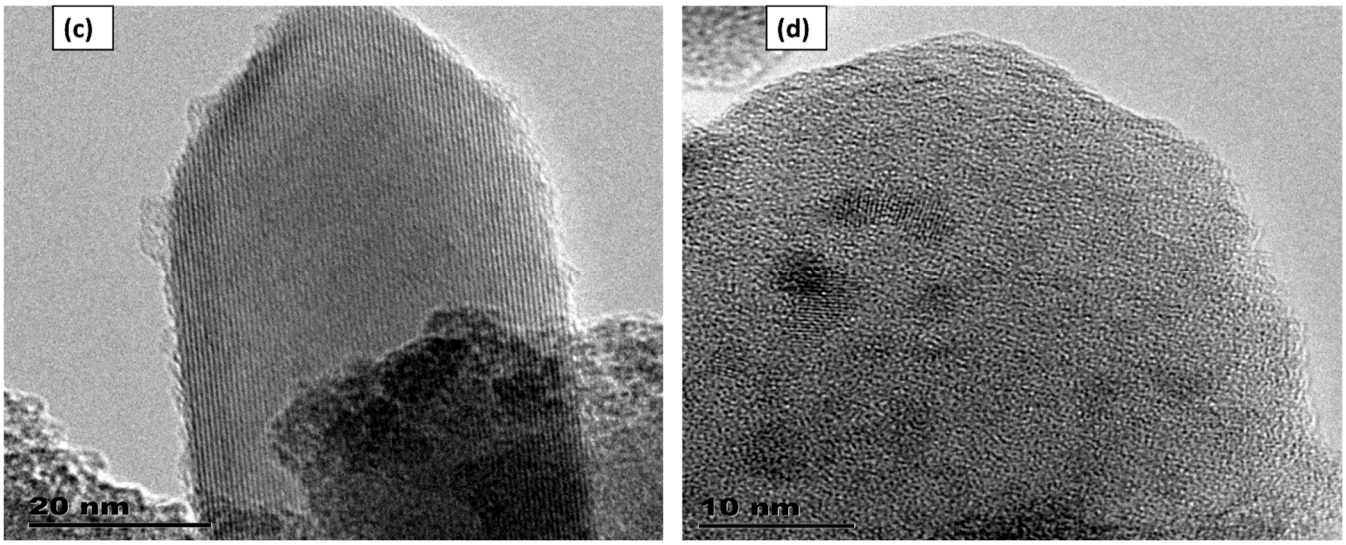

Figure 1. TEM image of Si-ZrO_2 nanoparticles.

Figure 2. HRTEM image of ZrO_2 and Si- ZrO_2 nanoparticles at higher magnification: SAED, Si-ZrO_2.

 doi:10.20944/preprints202409.2181.v

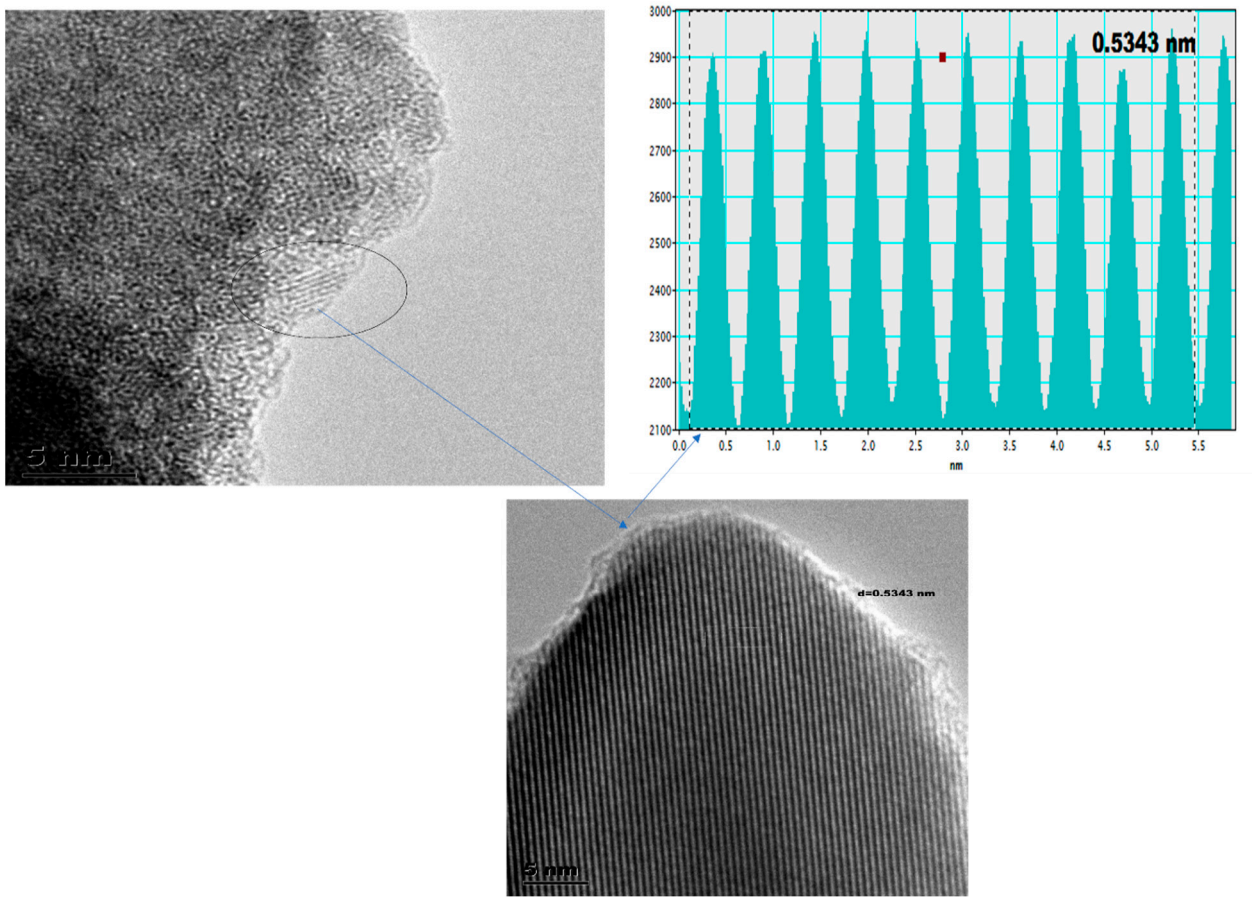

Figure 3. HRTEM lattice fringes of Si- ZrO_2.

Preprints.org (www.preprints.org) | NOT PEER-REVIEWED | Posted: 27 September 2024 doi:10.20944/preprints202409.2181.v

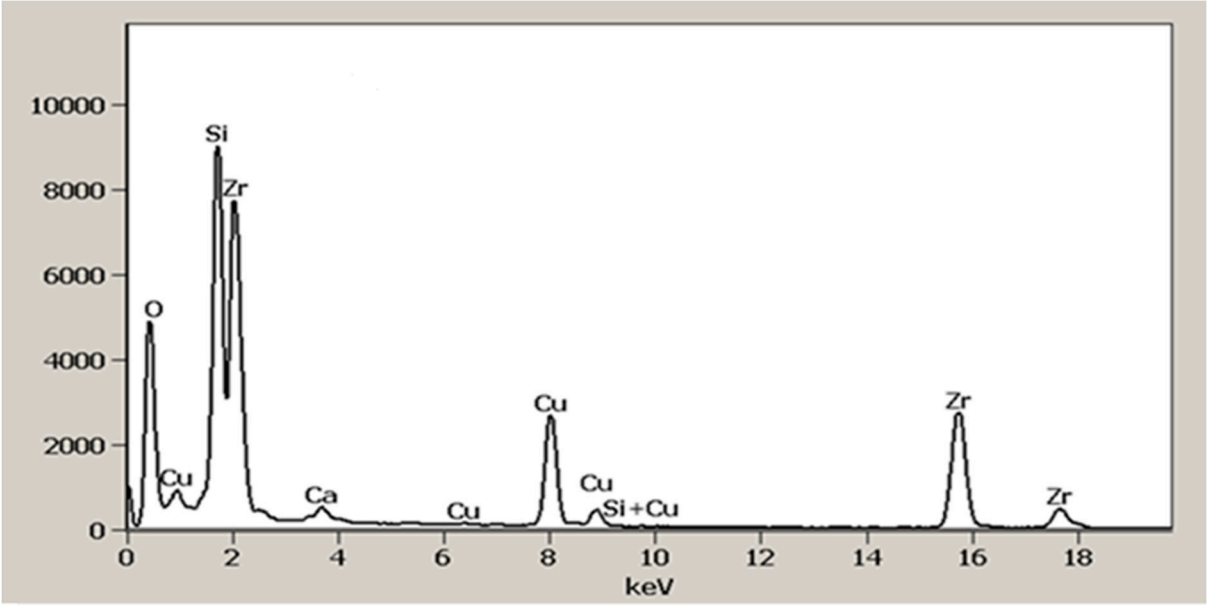

Element Line	Weight %	Weight % Error	Atom %	Atom % Error	Formula
O K	83.65	± 1.09	90.59	± 1.18	O
Si K	14.61	± 0.22	9.01	± 0.14	Si
Si L	---	---	---	---	(null)
Ca K	0.11	± 0.02	0.05	± 0.01	Ca
Ca L	---	---	---	---	(null)
Cu K	0.44	± 0.01	0.12	± 0.00	Cu
Cu L	---	---	---	---	(null)
Zr K	1.18	± 0.02	0.22	± 0.00	Zr
Zr L	---	---	---	---	(null)
Zr M	---	---	---	---	(null)
Total	100.00		100.00		

Figure 4. EDAX of Si- ZrO_2 nanoparticles.

3.2. Structural Analysis

Figure 5 shows the XRD results of Si-ZrO_2 nanoparticles. Identified phase of Si-ZrO_2 nanoparticles is monoclinic. Figure 5 show the transformation of amorphous silica to broader monoclinic zirconia peaks, this may be due to the calcination temperature of 600 °C. The obtained monoclinic is more thermodynamically stable phase where compared to tetragonal and cubic phases [18,22,24]. Figure 5 shows a broad monoclinic peak at 30.4°, which is in between 17° and 39°, due to amorphous silica phase. XRD peaks of the Si-ZrO_2 nanoparticles at 2 theta are 30.4°, 50.6°, 60.1° and 74.0° corresponding to the planes (1 1 1), (3 0 0), (1 3 1) and (4 1 1) as shown in Figure 5 [19]. This indicate the successfully synthesis of silica-zirconia nanoparticle in one pot as amorphous silica was transform to monoclinic structure of zirconia nanoparticles, this indicates that the silica core is well blend with zirconia [24].

 doi:10.20944/preprints202409.2181.v

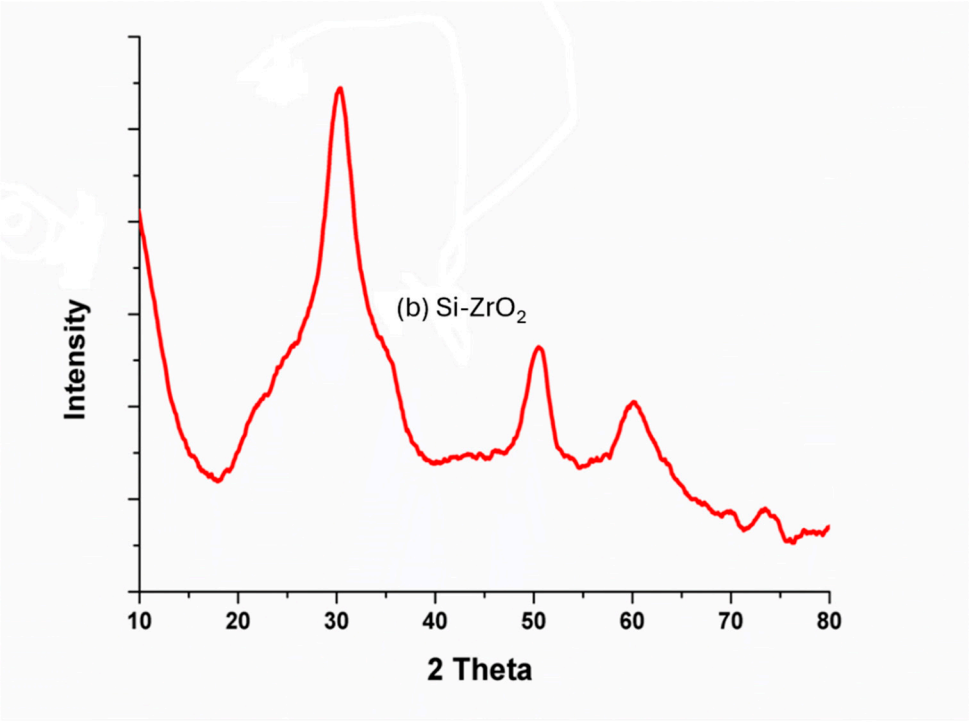

Figure 5. XRD patterns of Si-ZrO_2.

3.3. Scanning Electron Microscopy (SEM) Analysis

Figure 6 (a-b) shows the SEM morphology of the Si-ZrO_2 nanoparticles in 100 nm and 1 µm scale bar. Si-ZrO_2 nanoparticles shows a mixture of rod and spherical shapes with a diameter around 15 nm as shown in Figure 6 (a). which confirm by Lei Xu et.al results who obtained rod shape morphology with a diameter ranges between 150-200 nm [25].

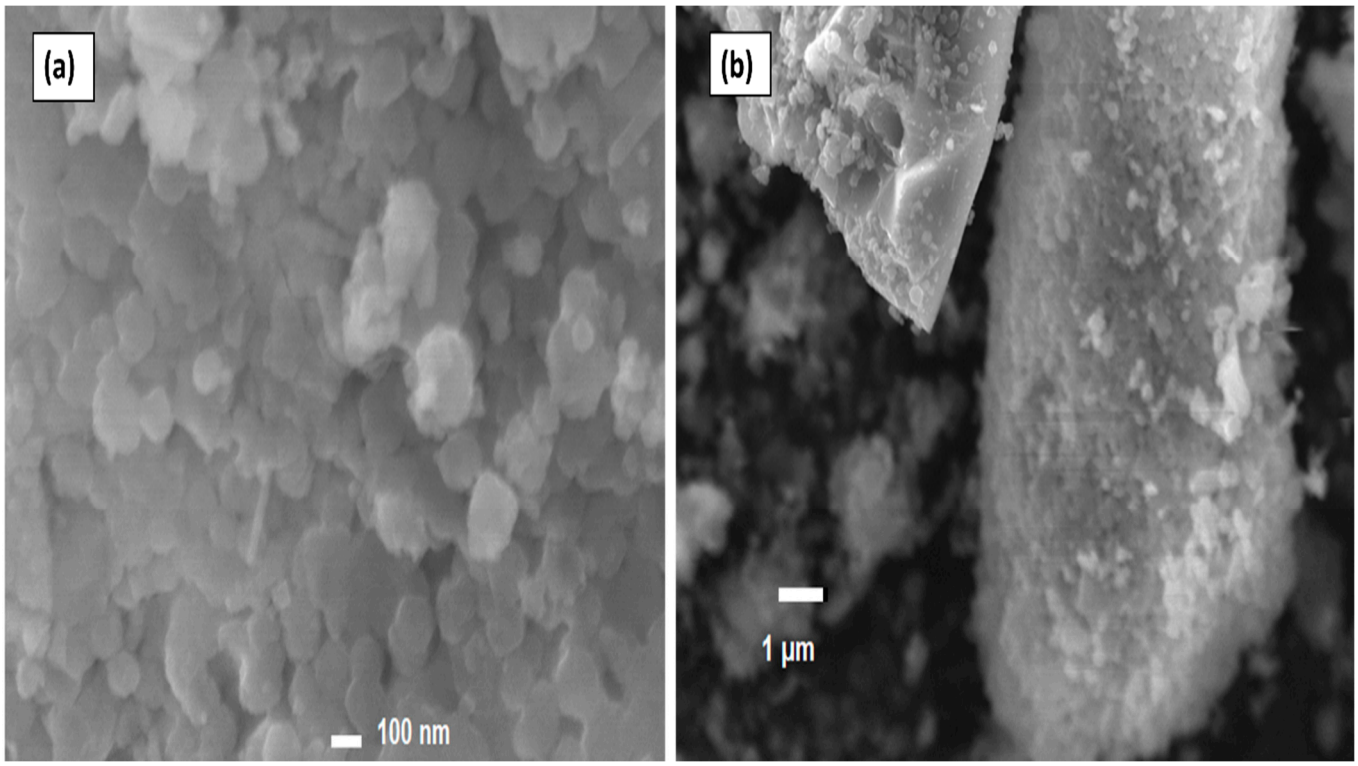

 doi:10.20944/preprints202409.2181.v

Figure 6. SEM: (a-b) Si-ZrO_2 nanoparticles.

3.4. TGA and Derivative Thermo-Gravimetric (DTG)

Figure 7 shows the TGA and DTG curve of Si-ZrO_2 nanoparticles. As seen in Figure 7, the thermal degradation has two weight loss stages. Figure 7 shows an initial weight loss of 4wt% between 40 °C and 100 °C, which caused by evaporation of adsorbed water. The second weight loss stage occurs between 150 °C and 900 °C, which is because of elimination of hydroxyl groups [18]. The TGA results shows that Si-ZrO_2 nanoparticles decompose less and remain stable at higher temperatures, with the total weight loss of 12%. DTG curves in Figure 7 confirms the two weight loss stages observed by TGA, with broad endothermic peaks between in the 100 °C to 300 °C due to desorbed water [26]. Furthermore, because of their low and steady thermal degradation, silica-zirconium nanoparticles are an ideal nanofiller for Nafion® membranes.

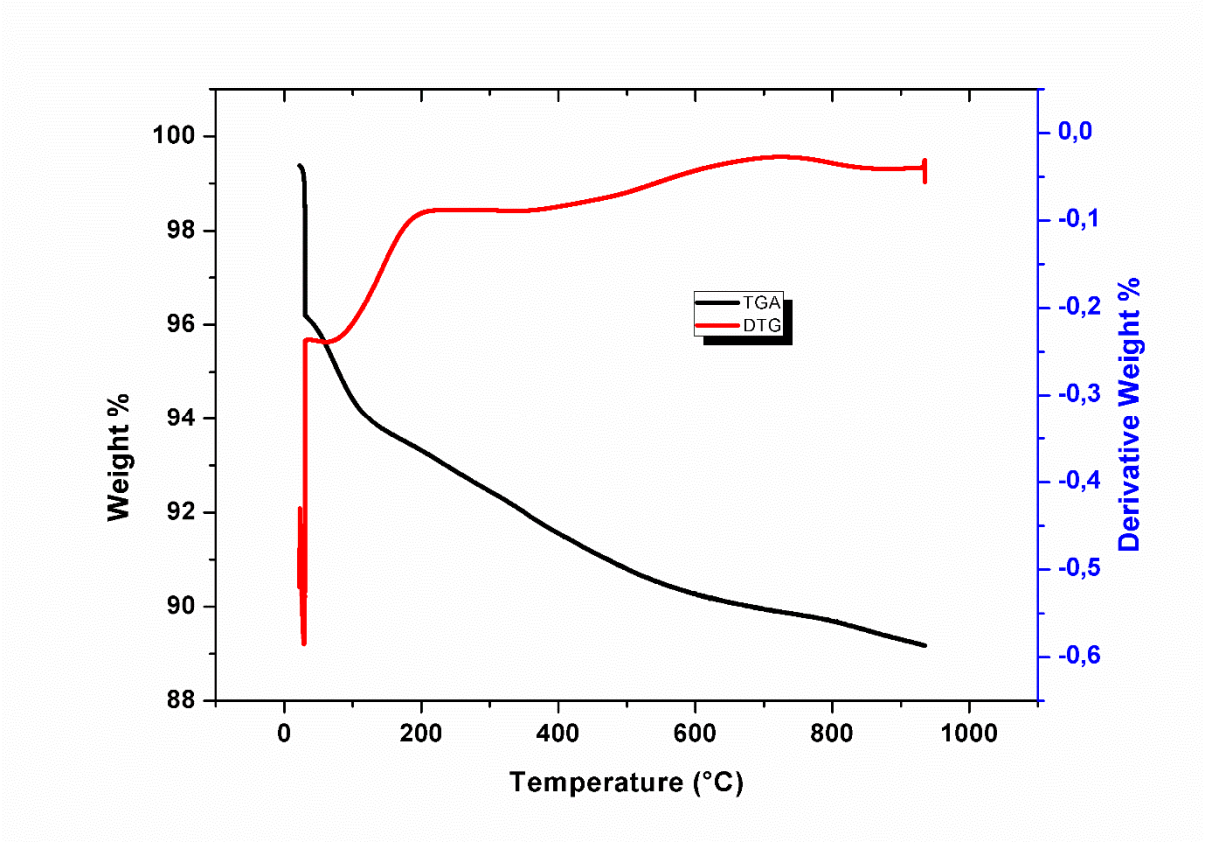

Figure 7. (A) TGA and DTG of Si-ZrO_2.

3.5. FTIR Spectrum of ZrO_2 Nanoparticles

FTIR results of Si-ZrO_2 nanoparticles is shown in Figure 8. The bands at 1627 cm^{-1}, 1062 cm^{-1} and 797 cm^{-1} attributed to symmetric stretching vibration Si-O-Si, this may be due to TEOS addition [27,28]. The absorption peaks observed at 1062 cm^{-1} and 945 cm^{-1} corresponds to the Si-O and Zr-O vibration bands generated by silica and zirconium raw materials [24,29]. The peak at 1452 cm^{-1} due to O-H bonding, and the peaks in the region of 1536 cm^{-1} may be due to the adsorbed moisture. The peaks at 2366 cm^{-1} corresponds Zr–OH stretching vibration bond indicate the present of zirconium nanoparticles. The peaks at 3411cm^{-1} attributed to O-H stretching vibration bands [28,29].

 doi:10.20944/preprints202409.2181.v

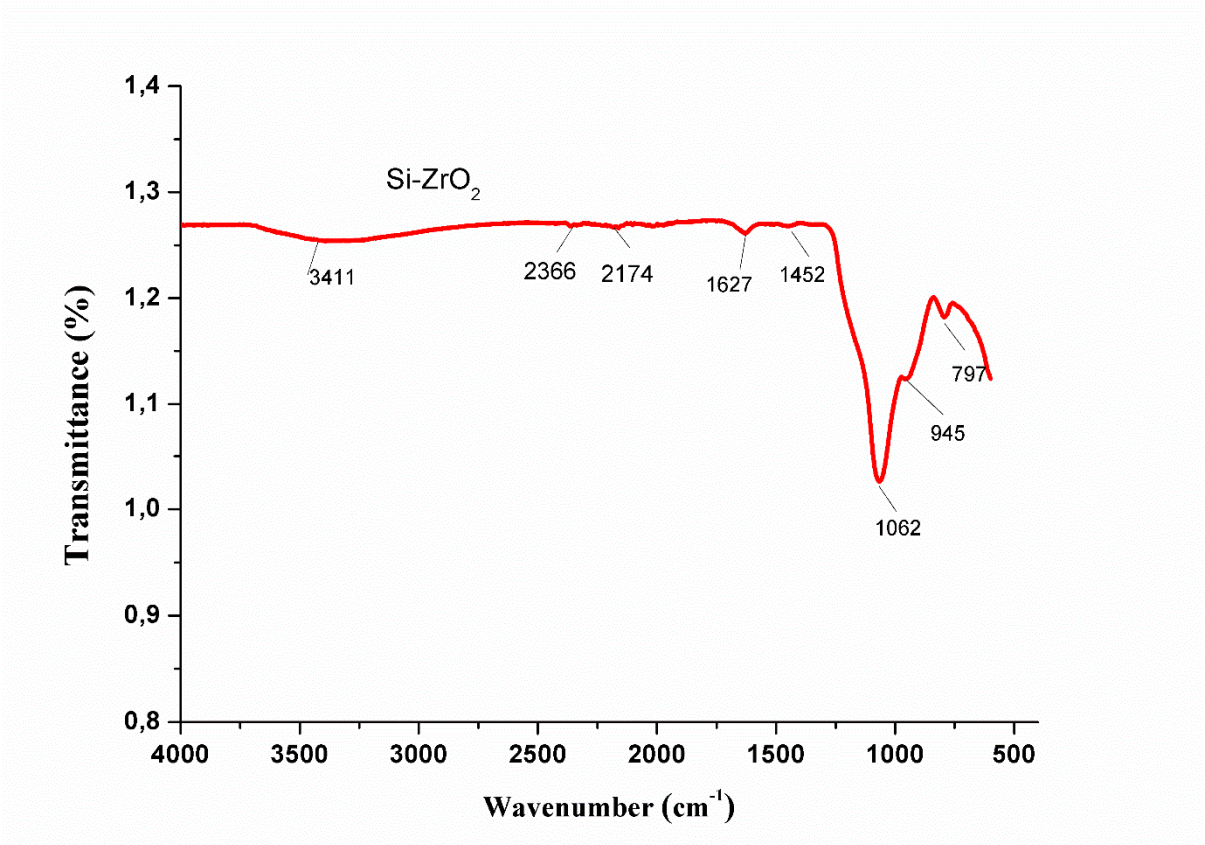

Figure 8. FTIR curves of Si-ZrO_2.

3.6. Nitrogen Adsorption-Desorption

Figure 9 and Table 1 show the BET-specific surface area of Si-ZrO_2 nanoparticles. Figure 9 shows that the effective diameter of the Si-ZrO_2 pores was reduced due to the incorporation of silica into the pores, which also resulted in the increase in the surface area [30]. BET results in Figure 9 (a-b) and Table 1 show that Si-ZrO_2 has a microporous structure with a higher surface area of 185 m^2/g. When the samples are aged at a higher temperature of 150 °C, the adsorption-desorption isotherm curves are type IV, with an H3 hysteresis loop, showing that the material has a mesoporous structure. Figure 9(b) shows that Si-ZrO_2 pore size distribution is narrower, with only one pore size distribution detected, this could be owing to the higher synthesis temperature. The pore distribution data indicate that ageing temperature has an impact on the porosity of zirconia nanoparticles. Si-ZrO_2 had pore volume of 0.14 cm^3/g as shown in Table 1. A. Bumajdad et al. got values greater than 144 m^2/g and 83 m^2/g [31,32]. This is due to the incorporation of tetraethyl orthosilicate into the zirconia solution.

 doi:10.20944/preprints202409.2181.v

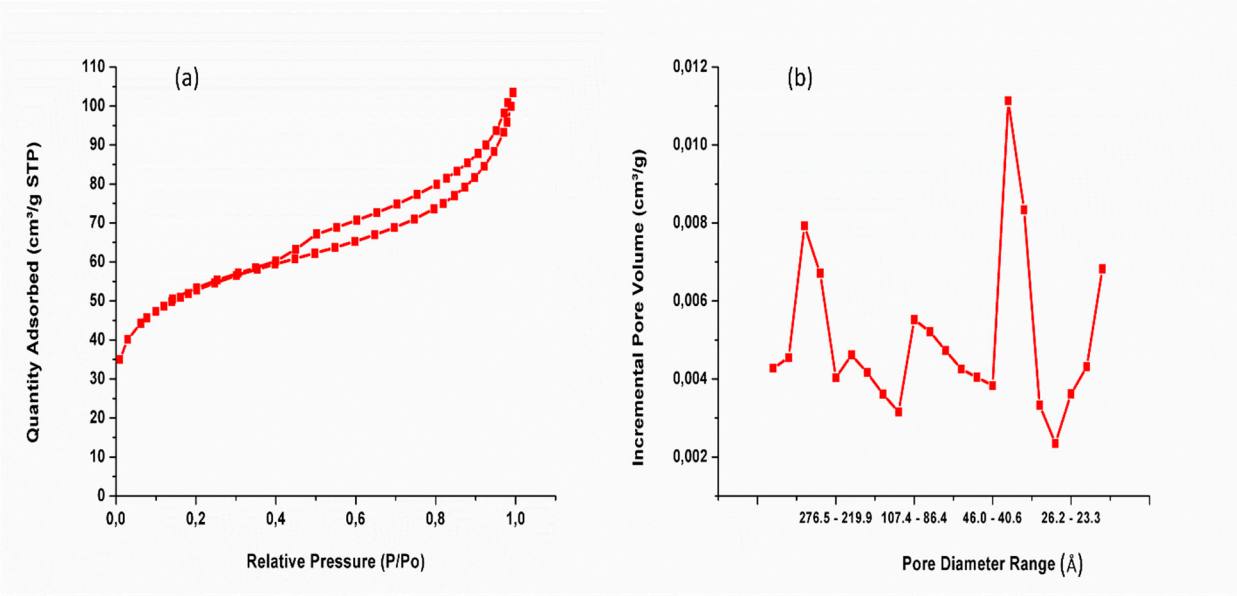

Figure 9. Pore size distribution curves of ZrO2 and Si-ZrO2 nanoparticles.

Table 1. BET of ZrO_2 nanoparticles: (a) Si-ZrO_2 and (b) ZrO_2.

Sample ID	Surface area (m^2/g)	Pore volume (cm^3/g)
Si- ZrO_2	185	0.14

3.7. Electrochemical Results

The cyclic voltammetry of Si-ZrO_2 is presented in Figure 10. The Si-ZrO_2 nanoparticle electrodes demonstrated characteristic electric double-layer capacitive behaviour with pseudo-rectangular voltametric diagrams in Figure 10. Figure 10 shows that increasing the scan rate from 10 mV s-1 to 100 mV s-1 increases the current due to resistance effects in the pores [18]. The volumetric cycle is higher and faster to complete with an increased electrode capacitance at 50 mV s-1 and 100 mV s-1 scan rates than at lower scan rates, demonstrating that the current reactivity of the Si-ZrO_2 electrode increased as the scan rate increases as shown in Figure 10. Furthermore, at increased scan rates of 100 mV s-1, Si-ZrO_2 had a greater area under the voltametric curve, and stronger charge transfer resistance [18] as shown in Figure 10. This could be because of Si-ZrO_2 large pores confirmed by BET. However, the quasi-rectangular shape, which is indicative of capacitive behaviour, increases dramatically between 50 and 100 mV s–1 which makes them suitable used in higher charge-discharge devices [33]

 doi:10.20944/preprints202409.2181.v

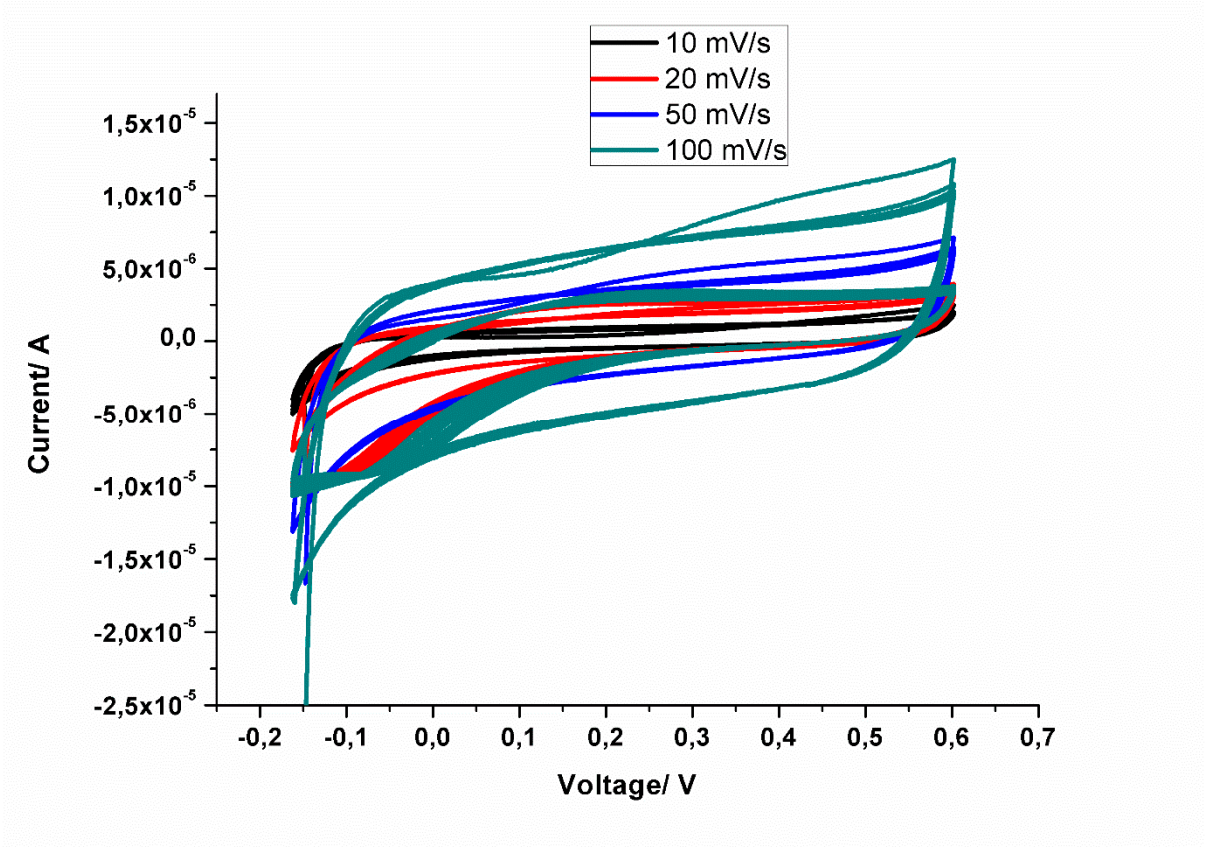

Figure 10. CV of Si-ZrO_2 in KCl electrodes at scanning rate of 10 mV s^{-1}, 20 mV s^{-1}, 50 mV s^{-1} and 100 mV s^{-1}.

The fundamental electrochemical behaviour of Si-ZrO_2 in 2M KCl electrolytes was investigated using the electrochemical impendence spectroscopy, as shown in Figure 11. Figures 11 and (insert) show the Nyquist plots for these cells over the frequency range of 100 kHz to 0.01 Hz. Si-ZrO_2 have vertical Nyquist plots without a curve zone, as seen in Figure 11 and (insert), due to electron transmission through their porous nanoparticle structure, which generally indicates excellent capacitive behaviour [34]. Figure 11 (insert) shows that at low frequencies, the curve is virtually vertical, showing optimal capacitive behaviour. The Si-ZrO_2 nanoparticles have a same low equivalent series resistance of only 6.25 Ohm, indicating better electrochemical performance in asymmetric devices due to increased electrolyte ion diffusion and mobility during charging and discharging cycles [33]. Furthermore, the huge surface area-to-volume ratio allows for a lot of charge accumulation, which leads to efficient charging. Such properties contribute to increased conductivity, making Si-ZrO_2 ideal for use in fuel cell applications.

 doi:10.20944/preprints202409.2181.v

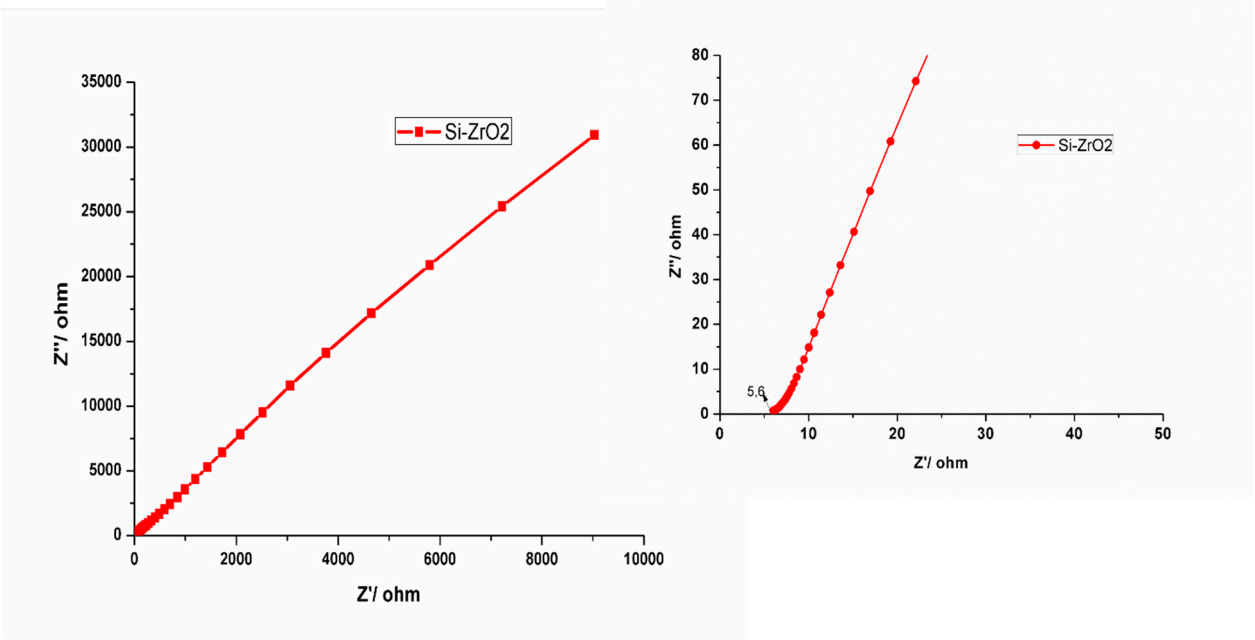

Figure 11. Nyquist plots of Si-ZrO_2 in KCl electrolytes at a range of 10 kHz–1Hz.

4. Conclusions

Si-ZrO_2 nanoparticles were well synthesised by precipitation method with higher crystalline and smaller particles of 5nm observed under HRTEM. The obtained results were supported by XRD which shows monoclinic phase and higher crystallinity with a broad peak due to amorphous silica nanoparticles. TGA results showed the ability of Si-ZrO_2 nanoparticles to be used under higher temperature applications as they started to degrade over 100 °C with less degradation up to 900 °C. The obtained FTIR results confirm the presence of silica and zirconia as Si-O and Zr-O bands observed. The BET results indicate that Si-ZrO_2 has higher surface area with the adsorption-desorption of type IV isotherm curves. The CV results show a higher redox peak which makes Si-ZrO_2 nanoparticles excellent nanofillers for composite membranes. The Nyquist plot of the Si-ZrO_2 nanoparticles shows a higher charge transmission resistance with excellent capacitance performances without diffusion constraints.

Acknowledgements: The authors are grateful to the CSIR for the TEM results. We also acknowledge the University of South Africa (AQIP) and National Research Foundation of South Africa for their financial support.

References

1. S. Anjum, S. Ishaque, H. Fatima, W. Farooq, C. Hano, B.H. Abbasi, I. Anjum, Emerging Applications of Nanotechnology in Healthcare Systems: Grand Challenges and Perspectives, Pharmaceuticals, 14 (2021) 707.
2. L. Fu, B. Wang, S.K.M. Sathyanath, J. Chang, J. Yu, K. Leifer, H. Engqvist, Q. Li, W. Xia, Microstructure of rapidly-quenched ZrO2-SiO2 glass-ceramics fabricated by container-less aerodynamic levitation technology. Journal of the American Ceramic Society, 106 (2023) 2635-2651.
3. S. Khan, S. Mansoor, Z. Rafi, B. Kumari, A. Shoaib, M. Saeed, S. Alshehri, M.M. Ghoneim, M. Rahamathulla, U. Hani, A review on nanotechnology: Properties, applications, and mechanistic insights of cellular uptake mechanisms. Journal of Molecular Liquids, 348 (2022) 118008.
4. S. Hassanzadeh-Tabrizi, Precise calculation of crystallite size of nanomaterials: A review. Journal of Alloys and Compounds, (2023) 171914.
5. H. Lin, C. Yin, A. Mo, Zirconia Based Dental Biomaterials: Structure, Mechanical Properties, Biocompatibility, Surface Modification, and Applications as Implant. Frontiers in Dental Medicine, 2 (2021) 689198.
6. A. Haleem, M. Javaid, R.P. Singh, S. Rab, R. Suman, Applications of nanotechnology in medical field: a brief review. Global Health Journal, 7 (2023) 70-77.

7. M.A. Ballem, J.M. Córdoba, M. Odén, Mesoporous silica templated zirconia nanoparticles. Journal of nanoparticle research, 13 (2011) 2743-2748.
8. S. Raj, M. Hattori, M. Ozawa, Ag-doped ZrO2 nanoparticles prepared by hydrothermal method for efficient diesel soot oxidation. Materials Letters, 234 (2019) 205-207.
9. D. Hidayat, A. Syoufian, M. Utami, K. Wijaya, Synthesis and Application of Na2O/ZrO2 Nanocomposite for Microwave-assisted Transesterification of Castor Oil. ICS Physical Chemistry, 1 (2021) 26-26.
10. P. Bansal, N. Kaur, C. Prakash, G.R. Chaudhary, ZrO2 nanoparticles: An industrially viable, efficient and recyclable catalyst for synthesis of pharmaceutically significant xanthene derivatives. Vacuum, 157 (2018) 9-16.
11. P. Sengupta, A. Bhattacharjee, H.S. Maiti, Zirconia: A Unique Multifunctional Ceramic Material. Transactions of the Indian Institute of Metals, 72 (2019) 1981-1998.
12. C. Verdi, F. Karsai, P. Liu, R. Jinnouchi, G. Kresse, Thermal transport and phase transitions of zirconia by on-the-fly machine-learned interatomic potentials. npj Computational Materials, 7 (2021) 156.
13. A.K. Chitoria, A. Mir, M. Shah, A review of ZrO2 nanoparticles applications and recent advancements. Ceramics International, 49 (2023) 32343-32358.
14. S.B. Matt, S. Raghavendra, M. Shivanna, M. Sidlinganahalli, D.M. Siddalingappa, Electrochemical Detection of Paracetamol by Voltammetry Techniques Using Pure Zirconium Oxide Nanoparticle Based Modified Carbon Paste Electrode. Journal of Inorganic and Organometallic Polymers and Materials, 31 (2021) 511-519.
15. S. Yilmaz, S. Cobaner, E. Yalaz, B. Amini Horri, Synthesis and Characterization of Gadolinium-Doped Zirconia as a Potential Electrolyte for Solid Oxide Fuel Cells. Energies, 15 (2022) 2826.
16. E. Gorbova, F. Tzorbatzoglou, C. Molochas, D. Chloros, A. Demin, P. Tsiakaras, Fundamentals and Principles of Solid-State Electrochemical Sensors for High Temperature Gas Detection. Catalysts, 12 (2021) 1.
17. F. Ahmadi, A. Sodagar-Taleghani, P. Ebrahimnejad, S.P.H. Moghaddam, F. Ebrahimnejad, K. Asare-Addo, A. Nokhodchi, A review on the latest developments of mesoporous silica nanoparticles as a promising platform for diagnosis and treatment of cancer. International Journal of Pharmaceutics, 625 (2022) 122099.
18. R. Sigwadi, T. Mokrani, M. Dhlamini, The synthesis, characterization and electrochemical study of zirconia oxide nanoparticles for fuel cell application. Physica B: Condensed Matter, 581 (2020) 411842.
19. R. Sigwadi, M.S. Dhlamini, T. Mokrani, P. Nonjola, Effect of Synthesis Temperature on Particles Size and Morphology of Zirconium Oxide Nanoparticle. Journal of Nano Research, 50 (2017) 18-31.
20. W.-S. Dong, F.-Q. Lin, C.-L. Liu, M.-Y. Li, Synthesis of ZrO2 nanowires by ionic-liquid route. Journal of colloid and interface science, 333 (2009) 734-740.
21. A. Kocjan, M. Logar, Z. Shen, The agglomeration, coalescence and sliding of nanoparticles, leading to the rapid sintering of zirconia nanoceramics. Scientific reports, 7 (2017) 2541.
22. N.D. Lestari, R. Nurlaila, N.F. Muwwaqor, S. Pratapa, Synthesis of high-purity zircon, zirconia, and silica nanopowders from local zircon sand. Ceramics International, 45 (2019) 6639-6647.
23. N.Y. Mostafa, Z. Zaki, Q. Mohsen, S. Alotaibi, A. Abd El-moemen, M.A. Amin, Carboxylate-assisted synthesis of highly-defected monoclinic zirconia nanoparticles. Journal of Molecular Structure, 1214 (2020) 128232.
24. S. Soontaranon, W. Limphirat, S. Pratapa, XRD, WAXS, FTIR, and XANES studies of silica-zirconia systems. Ceramics International, 45 (2019) 15660-15670.
25. L. Xu, H. Lei, Z. Ding, Y. Chen, R. Ding, T. Kim, Preparation of the rod-shaped SiO2@C abrasive and effects of its microstructure on the polishing of zirconia ceramics. Powder Technology, 395 (2022) 338-347.
26. H.-K. Min, Y.W. Kim, C. Kim, I.A. Ibrahim, J.W. Han, Y.-W. Suh, K.-D. Jung, M.B. Park, C.-H. Shin, Phase transformation of ZrO2 by Si incorporation and catalytic activity for isopropyl alcohol dehydration and dehydrogenation. Chemical Engineering Journal, 428 (2022) 131766.
27. S. Saravanan, R. Dubey, Synthesis of SiO2 nanoparticles by sol-gel method and their optical and structural properties. Romanian Journal of Information Science and Technology, 23 (2020) 105-112.
28. X. Lv, L. Yuan, C. Rao, X. Wu, X. Qing, X. Weng, Structure and near-infrared spectral properties of mesoporous silica for hyperspectral camouflage materials. Infrared Physics & Technology, 129 (2023) 104558.
29. Y. Liu, Y. Guo, Y. Zhu, D. An, W. Gao, Z. Wang, Y. Ma, Z. Wang, A sustainable route for the preparation of activated carbon and silica from rice husk ash. Journal of hazardous materials, 186 (2011) 1314-1319.
30. Y. Wu, Y. Xu, S. Li, L. Zhong, J. Wang, Y. Chen, High-surface-area mesoporous silica-yttria-zirconia ceramic materials prepared by coprecipitation method — the role of silicon. Ceramics International, 48 (2022) 21951-21960.
31. A. Bumajdad, A.A. Nazeer, F. Al Sagheer, S. Nahar, M.I. Zaki, Controlled Synthesis of ZrO2 Nanoparticles with Tailored Size, Morphology and Crystal Phases via Organic/Inorganic Hybrid Films. Scientific reports, 8 (2018) 3695.

 doi:10.20944/preprints202409.2181.v

32. C.V. Reddy, B. Babu, I.N. Reddy, J. Shim, Synthesis and characterization of pure tetragonal ZrO2 nanoparticles with enhanced photocatalytic activity. Ceramics International, 44 (2018) 6940-6948.
33. S. Khalid, C. Cao, L. Wang, Y. Zhu, Microwave Assisted Synthesis of Porous NiCo2O4 Microspheres: Application as High Performance Asymmetric and Symmetric Supercapacitors with Large Areal Capacitance. Scientific reports, 6 (2016) 22699.
34. L.-P. Lv, Z.-S. Wu, L. Chen, H. Lu, Y.-R. Zheng, T. Weidner, X. Feng, K. Landfester, D. Crespy, Precursor-controlled and template-free synthesis of nitrogen-doped carbon nanoparticles for supercapacitors. RSC Advances, 5 (2015) 50063-50069.